



Construction of a Tephra-Based Multi-Archive Coherent Chronological Framework 1 for the Last 2 Deglaciation in the Mediterranean Region

L. Bazin, B. Lemieux-Dudon, G. Siani, A. Govin, A. Landais, D. Genty, E. Michel, S. Nomade

► To cite this version:

L. Bazin, B. Lemieux-Dudon, G. Siani, A. Govin, A. Landais, et al.. Construction of a Tephra-Based Multi-Archive Coherent Chronological Framework 1 for the Last 2 Deglaciation in the Mediterranean Region. *Quaternary Science Reviews*, 2019, 216, pp.47-57. 10.1016/j.quascirev.2019.05.018 . hal-03089446

HAL Id: hal-03089446

<https://cnrs.hal.science/hal-03089446>

Submitted on 28 Dec 2020

HAL is a multi-disciplinary open access archive for the deposit and dissemination of scientific research documents, whether they are published or not. The documents may come from teaching and research institutions in France or abroad, or from public or private research centers.

L'archive ouverte pluridisciplinaire **HAL**, est destinée au dépôt et à la diffusion de documents scientifiques de niveau recherche, publiés ou non, émanant des établissements d'enseignement et de recherche français ou étrangers, des laboratoires publics ou privés.

Construction of a Tephra-Based Multi-Archive Coherent Chronological Framework for the Last Deglaciation in the Mediterranean Region

L. Bazin¹, B. Lemieux-Dudon², G. Siani³, A. Govin¹, A. Landais¹, D. Genty¹, E. Michel¹, S. Nomade¹

¹ Laboratoire des Sciences du Climat et de l'Environnement, LSCE/IPSL, CEA-CNRS-UVSQ, Université Paris-Saclay, 91191, Gif-sur-Yvette, France

² Centro Euro-Mediterranea sui Cambiamenti Climatici, Bologna BO, Italy

³ GEOPS UMR 8148 CNRS, Université Paris Sud and Paris Saclay, Orsay, France

Abstract

Proxy records from different climate archives such as ice cores, speleothems or sediment cores are essential to define the sequence of events over to the last deglaciation. However, multi-archive comparison and compilation of data, necessary to assess the robustness of climate models, are rapidly limited by inconsistencies between archives' chronology. Here we present the development and validation of the Datice chronological integration tool for the construction of multi-archive coherent chronologies. This chronology building tool, first developed to date ice cores only, can now integrate deposition-like archives such as sediment cores and speleothems, independently or coherently. The robustness of this dating method resides in its capacity to build coherent chronologies for multiple archives with a proper calculation of chronological uncertainties. Using this tool, we were able to construct a coherent chronology for the last deglaciation in the Mediterranean region based on volcanic tephra layers correlation in terrestrial and marine sediment cores. We confirm the synchronicity, within chronological errors, of the sequence of events characterizing the last deglaciation between Greenland and the Mediterranean region, independently of any climatic alignment assumptions. Using this chronological framework, we however highlight some regional expression of this transition period in term of vegetation cover over the Mediterranean region.

Key words: last deglaciation, Mediterranean region, multi-archive comparison, coherent chronology, tephra, vegetation changes.

1. Introduction

Understanding the mechanisms driving climate changes at the Earth's surface has largely benefited from measurements of geochemical tracers from various climate archives. Marine cores have provided a first relatively precise timing of reference for the succession of glacial and

interglacial periods over the last millions of years (Imbrie and Imbrie, 1980). Later on, polar ice cores were the first to clearly evidence the abrupt climate variability characterizing the last glacial period (Dansgaard-Oeschger events, Dansgaard et al., 1993). Concomitantly, marine cores from North Atlantic revealed the occurrence of strong iceberg-rafter episodes during the last glacial period, named Heinrich events, that are related to some Dansgaard-Oeschger events (Heinrich, 1988). Since this pioneer period in paleoclimatology, many different archives from the continent and the ocean have recorded the succession of glacial and interglacial periods as well as the millennial-scale climate variability of the last glacial periods (Martrat et al., 2004; Jouzel et al., 2007; Cheng et al., 2009). Obtaining records from different latitudes is essential to accurately depict the regional as well as global variability associated with past climate changes. With the improvement of climate models (Eyring et al., 2016), it is becoming clear and necessary to combine records from different archives in order to further assess the robustness of model outputs and their capacity to reproduce the duration and pace of past climate changes at different spatial scales (Kageyama et al., 2018).

Efforts have been made to combine records of marine and continental origin covering the last deglaciation (Clark et al., 2012; Shakun et al., 2012; Moreno et al., 2014). This period framed between 19 and 11 ka ago corresponds to the transition between the last glacial period and the current interglacial (i.e. Holocene). It was induced by changes in insolation, associated with changes in greenhouse gases (GHG) concentration, atmospheric and ocean circulation reorganisations as well as the melting of polar ice sheets. The last deglaciation is widely recorded within various paleoclimatic archives. Even if numerous radiocarbon ages constrain the sequence of events of this key period, the absolute timing of changes is not always consistent from one site to another essentially because of the spatial and temporal variability of reservoir ages, the calibration of the ^{14}C dates (Siani et al., 2001; Reimer et al., 2013), but also the sample selection (e.g. shells, wood, bulk sediment; Müller et al., 2011). The combination of climate data compilations and model simulations generally agree with the major role of GHGs and Atlantic Meridional Overturning Circulation (AMOC) variations during the last deglaciation. However, the relative leads and lags between different regions and/or type of paleoclimate archives remain difficult to assess and therefore largely unknown. Indeed, even if efforts were made in order to calibrate ^{14}C dates on the same reference curves (Clark et al., 2012; Shakun et al., 2012), the harmonization of chronologies between the ocean and the continent, when it exists, remains largely based on alignment assumptions. For example, Moreno et al., (2014) have combined terrestrial records covering the period 60-8 ka from lake sediments, speleothems, an ice core and pollen records from marine cores. They choose not to revise the published age models. However, most of the marine cores included in their compilation possess chronologies derived from the alignment of their surface records (planktonic foraminifera

$\delta^{18}\text{O}$ or Sea Surface Temperature - SST) with a Greenland reference record ($\delta^{18}\text{O}_{\text{ice}}$ of NGRIP usually). While such an assumption can be easily verified close to Greenland, thanks to the numerous volcanic ash layers (Davies et al., 2010; Austin and Hibbert, 2012), it can be questionable down to the Iberian margin and the Mediterranean region, especially when there is no assessment of the synchronization uncertainty.

Here we propose an assessment of relative climate changes associated with the last deglaciation using a coherent chronological framework based on tephra layers that are used as anchors to synchronize records. These volcanic derived deposits are by nature independent from climatic alignment assumptions (e.g. Lane et al., 2013; Lowe et al., 2015). In order to verify the consistency of the timing of changes associated with this transition, we primarily focus our chronological efforts on the Mediterranean region (Figure 1), which presents two main advantages. First, it offers a large variety of climatic records obtained from different archives on the continent and from the sediments of the Mediterranean Sea. Second, this region is characterized by widely dispersed tephra layers found within both continental and marine sedimentary archives. Their geochemical characteristics allow us to identify common tephra horizons in different archives (Albert et al., 2017). In some cases these tephra layers are even precisely and accurately dated using the $^{40}\text{Ar}/^{39}\text{Ar}$ method (Galli et al., 2017; Giaccio et al., 2017; Albert et al., 2019), or by ^{14}C dating of the surrounding material (Lee, 2013; Albert et al., 2015; Bronk Ramsey et al., 2015).

The consistency between chronologies of the different Mediterranean paleoclimate archives included in our study is obtained using the Datice **chronological integration tool** (Lemieux-Dudon et al., 2010). Datice was initially developed for coherent ice core dating, and used to produce the reference chronology of ice cores (Antarctic Ice Core Chronology - AICC - 2012, Bazin et al., 2013; Veres et al., 2013). For the purpose of our study, we improved the Datice chronological integration tool and developed a multi-archive version allowing us to consistently build chronologies for sediment cores and speleothems in addition to ice cores.

The article is organized as follows. First we present the Datice Multi-archive tool and its new development to build chronologies for deposition-like archives. Second, we list the different sites included in this study and explain the rationale behind the construction of a tephra-based chronological framework for the last deglaciation in the Mediterranean region. The comparison of our coherent chronology with previously published age scales highlights the strength and usefulness of the Datice tool for multi-archive compilation applications. Finally, we discuss the coherency of

climatic changes as recorded by different archives within the Mediterranean region and compare them with NGRIP $\delta^{18}\text{O}_{\text{ice}}$ reference record from Greenland.

2. Tools

We use the Datice chronological integration tool to build a multi-archive coherent chronology (<https://datice-multi-archives.ipsl.fr/>). Information on where and how to install Datice are given in a dedicated paragraph at the end of the article. Datice was initially developed to produce coherent chronologies for ice cores by integrating absolute and relative age constraints between several ice cores for both the ice and gas phases (Lemieux-Dudon et al., 2010; Buiron et al., 2011; Bazin et al., 2013; Veres et al., 2013). Following this work, additional developments were necessary to constrain annually resolved archives such as the Greenland ice cores back to 60 ka (GICC05 chronology, Andersen et al., 2006; Rasmussen et al., 2006; Vinther et al., 2006; Svensson et al., 2008), and led to the integration of duration constraints (Lemieux-Dudon et al., 2015). On a mathematical point of view, Datice is an inverse modelling method based on Bayesian statistics. It makes the best compromise between an initial age-depth model, and its associated uncertainty estimation, with absolute and relative age constraints obtained at various depths. The prior chronology is deduced from the integration with depth of background parameters and corresponding uncertainties, all defined by the user (Table 1). Taking into account the chronological constraints (i.e. all background parameters and age markers) of all sites, as well as the stratigraphic links defined across sites, Datice produces a single chronology that is coherent to all sites and benefits from a proper assessment and propagation of age uncertainties. Moreover, after obtaining the final chronology, uncertainties are also propagated to the parameters used to calculate the final age for the different archives (e.g. accumulation rate, deposition rate, thinning function, Lock-in depth).

For ice core dating, it is necessary to date both the ice and gas phases. In Datice, the prior ice chronology is calculated from given scenarios of snow accumulation and thinning function, while the gas chronology is deduced from the evolution with depth of the reconstructed lock-in depth (i.e. the depth at which the air is trapped within the ice lattice, typically 50-100 m under the surface, Table 1, Lemieux-Dudon et al., 2010).

For the purpose of multi-archive coherent dating, we further developed a new version of Datice in order to extent the use of this tool to date paleoclimate archives such as speleothems and (terrestrial and marine) sediment cores. For these mono-phase archives, the age calculation is simpler than for ice cores. Contrary to ice, which is formed from the compaction of snow and continues to thin during burying, speleothems are not affected by post-depositional compaction

effects. For sediment cores, compaction effects are generally not taken into account due to the difficulty to properly quantify or model them. Consequently, the age-depth relationship for such climate archives (i.e. speleothems and sediment cores) is directly obtained from the integration with depth, **from the top to the current depth**, of the deposition rate $L(z)$ (e.g. the growth rate for speleothems or the sedimentation rate for marine or lake sediment cores in **centimetres per year**; equation 1).

$$Age(z) = \int_0^z \frac{1}{L(z')} dz' \quad (1)$$

As the age is parameterised as increasing with depth, the depth reference is taken at the surface of the sediment or the top of the speleothem. Similarly to the background parameters for ice cores, the error of the prior estimation of the deposition rate can be parameterised as constant or varying with depth. So far, Datice Multi-archive **can only** integrate continuous archives. When dealing with hiatuses (regardless of the type of archives), each section has to be integrated separately (before and after the hiatus). **Users have the possibility to associate error correlation with the prior estimation of the deposition rate. Adding such an error correlation allows Datice Multi-archive to propose a final deposition rate with smoother variations than in the case of no error correlation (Table 1).**

In order to obtain precise and coherent chronologies, different sets of markers can be included in Datice Multi-archive (Table 1). Some are specific to ice cores, such as gas age markers or gas stratigraphic links. However, the markers applied to the ice phase (e.g. age markers, duration constraints, stratigraphic links) can also be applied to the deposition-like archives. The uncertainty associated with all markers must be given in years and should take into account all sources of error (e.g. the identification of markers, resolution of data, measurement uncertainties, calibration). **Ages deduced from ^{14}C measurements should be calibrated into calendar years before their integration into Datice Multi-archive.** Datice Multi-archive **can also** add error correlation between different sets of markers if needed. The coherency of the chronology between the sites is ensured by the integration of stratigraphic links. These markers must be defined *a priori* between two cores and have to be associated with an uncertainty in years. The final chronology uncertainty calculated by Datice Multi-archive is then a compromise between the uncertainties of the background chronology and all age markers. Large uncertainties associated with the background parameters (e.g. sedimentation rate, accumulation rate, thinning function, Table 1) necessarily result in a large uncertainty for the prior chronology. When such large uncertainties occur, the optimisation module of Datice Multi-archive has sufficient freedom to modify accordingly the background parameters and

the chronology to fit the more robust dating constraints (i.e. the age markers and the stratigraphic links). Inversely, when we are confident in our background parameters, the final chronology will remain close to its initial age-depth model.

Datice Multi-archive is a complementary tool to the already existing applications used to date paleoclimate archives. The other Bayesian tools such as OxCal, BChron or Bacon (Haslett and Parnell, 2008; Bronk Ramsey, 2009; Blaauw and Christeny, 2011; Parnell et al., 2011), are not suited for the specific problematic of ice core dating, but they offer the possibility to calibrate ^{14}C ages as well as build consistent chronologies for sediment cores and/or speleothems (Bronk Ramsey et al., 2014, 2015). On the other hand, IceChrono (Parrenin et al., 2015) builds coherent chronologies for ice cores only, similarly to the previous Datice version. Thanks to our recent developments, Datice Multi-archive is the only chronological tool allowing to build coherent chronologies for ice cores as well as other paleoclimatic archives such as speleothems or (terrestrial and marine) sediment cores. Datice Multi-archive offers an easy way to parameterize the relative constraints between the different archives through the implementation of the stratigraphic links with the possibility of adding error correlation between markers.

Consequently, the strength of Datice Multi-archives when building chronologies for paleoclimatic archives is its capacity to reconstruct chronologies for ice cores and deposition-like archives, with the proper transfer of uncertainties. Datice Multi-archive is therefore especially useful when addressing questions about the relative timing of changes associated with major climatic events that are recorded by proxies from multiple sites and archives, such as in the case of the last deglaciation.

Table 1: input parameters required for Datice Multi-archive

Background parameters			Age markers
Ice cores	Sediment cores	Speleothems	Absolute ages
Accumulation rate	Sedimentation rate	Deposition rate	Duration constraints
Thinning function			Stratigraphic links
Lock-in depth			(+ gas absolute ages, gas stratigraphic links, delta-depth markers, all specific for ice cores)
+ associated uncertainties for each parameter and each dating constraint			
(possibility of adding error correlations for paired markers)			

3. Material and Methods

To test this new Datice version, we choose to integrate paleoclimate archives from the Mediterranean region that cover continuously the last deglaciation. The selected archives were taken on the continent (speleothems and lake/peat sediments), and from the Mediterranean Sea, and exhibit multiple high-resolution proxies. The selected marine and lake sediment cores present numerous common and independently dated tephra layers (Figure 2). This unique set of chronological tie points is of key importance to safely discuss the relative changes between the sediment records without any assumption of climatic synchronicity, as usually implied in case of chronological alignment. Consequently, we selected one marine core (MD90-917), three continental sediment cores (Monticchio, Ohrid, Tenaghi Philippon) and two speleothems (Sofular, La Mine) spread over the Mediterranean perimeter (Figure 1, Table 2). The two selected speleothems, while being independently dated and not integrated in our tephra-based Mediterranean coherent chronological framework, bring complementary information about the expression of the last deglaciation within the Mediterranean region. They, moreover, serve as test cases to validate the developments and use of Datice Multi-archive to date deposition-like archives (see section 4.1). We summarized in Table 2 the independent radiometric constraints and relative tie-points available for each site.

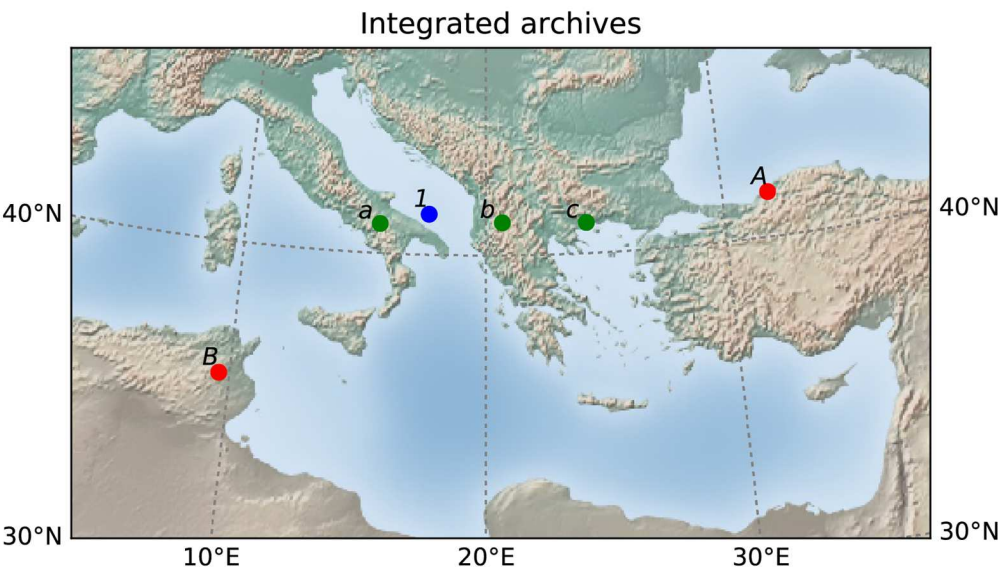
Both speleothems chronologies are based on numerous ^{230}Th ages (Genty et al., 2003; Fleitmann et al., 2009; Göktürk et al., 2011). For Monticchio, three tephra layers corresponding to ashes from the Somma-Vesuvius volcanic field have been historically recognised and are associated with a 1-sigma uncertainty of 1 year ("*" in Figure 2). The absolute ages of the Mercato and Y2 tephra layers were obtained after combining together numerous ^{14}C calibrated ages from different archives (Zanchetta et al., 2011; Lee, 2013; Bronk Ramsey et al., 2015). This method statistically reduces the uncertainty associated with one volcanic event that is well-identified and ^{14}C -dated in numerous paleoclimate archives, especially when no $^{40}\text{Ar}/^{39}\text{Ar}$ date is available. The remaining absolute ages correspond to $^{40}\text{Ar}/^{39}\text{Ar}$ dates obtained on inland deposits of well-known eruptions ("°" in Figure 2, Pappalardo et al., 1999; Galli et al., 2017; Giaccio et al., 2017; Albert et al., 2019). As their published ages were obtained from different calibrations, we decided to homogenize all the $^{40}\text{Ar}/^{39}\text{Ar}$ ages. Ages are then recalculated using the more recent ACs-2 standard of Niespolo et al., (2017) (1.1891 Ma), and based on the ^{40}K total decay constant of Renne et al., (2011) that is independent from astronomical tuning (Figure 2). Consequently, the corresponding ages used in this work, and presented in Figure 2, may slightly differ from the published ages due to this homogenization and recalibration process (see supplementary material). Including the recent work of Albert et al., 2019, all three major eruptions of the Campi Flegrei (i.e. NYT, Y3, Y5) that are recognised at the different sites are now precisely and

accurately dated by $^{40}\text{Ar}/^{39}\text{Ar}$. They all remain in good agreement with the ^{14}C ages previously published.

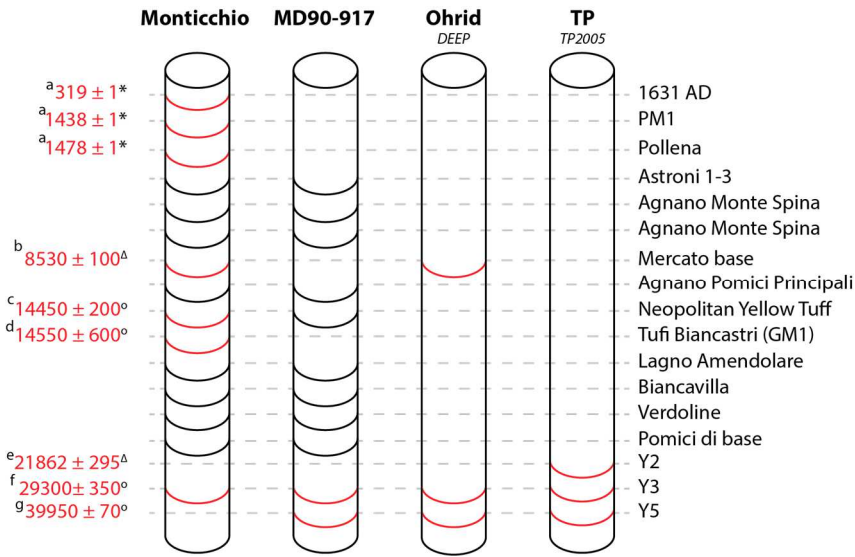
Finally, the chronological coherency of all sediment cores is assured by the identification of common tephra layers, which transfer the absolute age of an independently and better dated record to a poorly dated one (Figure 2). The identifications and correlation of the tephra layers are based on the published geochemical composition of tephra and their already proposed correlations (Siani et al., 2001, 2004, Wulf et al., 2004, 2008, 2018, Tomlinson et al., 2012, 2014; Leicher et al., 2016; Albert et al., 2019). We further confirmed these assignments using the RESET database (Lowe et al., 2015). We assigned an uncertainty of 1-year to these volcanic stratigraphic links. Tephra deposition after an eruption can be considered instantaneous (i.e. <1 year). While we may encounter some bioturbation perturbation in the top-most centimetres of the sediment locally, the chronological error associated to this parameter remains difficult to model and quantify (Bard et al., 1987; Manighetti et al., 1995; Carey, 1997; Charbit, 2002; Barsanti et al., 2011). However, enlarging the uncertainty of our volcanic-based stratigraphic links up to 10 years to account for these potential perturbations do not affect significantly the final chronology (not shown). Such a test gives us confidence in the tephra-based chronology using a 1-year uncertainty associated to the tephra correlation.

To summarize, our coherent chronological context of the last deglaciation in the Mediterranean region is constrained by 53 independently dated age markers and 20 relative stratigraphic links (Table 2 and Figure 2) for the sediment cores. Additional 59 and 13 absolute age markers constrain the Sofular and La Mine speleothem chronologies respectively, which remain here independent from the tephra-based common chronology.

To complete the set of *a priori* parameters (Table 1), we need to propose a prior estimation of the sedimentation/deposition rates and associated uncertainties for each deposition-like archive integrated into Datice Multi-archive. Ideally these estimates have to be independent from the age constraints, which is not always achievable. For Monticchio, we deduced the prior sedimentation rate from its published varved chronology covering the last deglaciation (Allen et al., 1999) and assigned a 10% uncertainty, as proposed in the original paper (Table 3). For the other Mediterranean archives, no prior estimation of the sedimentation rate independent from the absolute age markers were available. Consequently we decided to estimate a constant background sedimentation rate from the linear regression of all the age markers for each site and associated it with a large constant uncertainty ($\geq 50\%$, Table 3). Such a parameterization allows Datice Multi-archive to substantially modify the background chronology and, as a result, respect the collection of age constraints. The chronology produced by Datice then better agrees with the age markers than with the prior guess.



252 Figure 1: Map of all the sites discussed in this study. Speleothems are in red (A - Sofular, B - La Mine),
253 lake/peat sediments are in green (a - Monticchio, b - Ohrid, c - Tenaghi Philippon) and the MD90-917
254 marine core is in blue (1). All identifications are consistent with Table 2.



256 Figure 2: Common and well-dated tephra layers in the Mediterranean region identified in the
257 selected terrestrial and marine sediment cores (Monticchio, MD90-917, Ohrid and Tenaghi Philippon
258 – TP, (Siani et al., 2001, 2004, Wulf et al., 2004, 2008, 2018, Tomlinson et al., 2012, 2014; Lowe et al.,
259 2015; Leicher et al., 2016; Albert et al., 2019). Tephra in red are absolutely dated with the reference

year of 1950 AD (* Somma-Vesuvius historical eruption, $^{40}\text{Ar}/^{39}\text{Ar}$ dates or $^{\Delta}$ average ^{14}C ages with 1-sigma errors). For more consistency, all $^{40}\text{Ar}/^{39}\text{Ar}$ ages are recalculated using the more recent ACs-2 standard and the ^{40}K total decay constant independent from astronomical calibration (Renne et al., 2011; Niespolo et al., 2017). Ages can therefore slightly differ from the original publications cited here. References : a - Wulf et al., 2008, b - Zanchetta et al., 2011, c - Galli et al., 2017, d - Pappalardo et al., 1999, e - Bronk Ramsey et al., 2015, f - Albert et al., 2019, g - Giaccio et al., 2017.

Table 2: List of Mediterranean sites and age constraints considered here for the last deglaciation.

ID	Name	Lat. (°N)	Long. (°E)	Absolute markers	Stratigraphic links (relative)	References
1	MD90-917	41.00	17.52	25 ^{14}C cal. ages 2 tephras	10 to Monticchio 3 to TP 2 to Ohrid	Siani et al., 2001, 2004, 2010; this study
a	Monticchio	40.93	15.58	3 historical eruptions 4 tephras	10 to MD90-917 2 to Ohrid 1 to TP	Allen et al., 1999; Wulf et al., 2008
b	Ohrid	41.03	20.7	3 tephras	2 to Monticchio 2 to TP 2 to MD90-917	Francke et al., 2016
c	Tenaghi Philippon (TP)	40.97	24.22	13 ^{14}C cal. ages 3 tephras	2 to Ohrid 3 to MD90-917 1 to Monticchio	Müller et al., 2011; Wulf et al., 2018
A	Sofular	41.42	31.93	59 U/Th ages		Fleitmann et al., 2009; Göktürk et al., 2011
B	La Mine	35.83	9.58	13 U/Th ages		Genty et al., 2006

Table 3: Values of constant sedimentation rates and corresponding errors used as background parameters in Datice Multi-archive.

	MD90-917	Monticchio	Ohrid	Tenaghi Philippon	Sofular	La Mine
Sed. rate (cm/a)	0.0346	Varved chronology ^a	0.04	0.0338	0.008	0.001
Sigma (cm/a)	0.015	10%	0.02	0.02	0.01	0.01

^aAllen et al., 1999

4. Results

4.1. Datice chronologies of deposition-like archives

We validate Datice Multi-archive developments to build chronologies for deposition-like archives, such as speleothems and sediment cores, using the Tunisian speleothem of La Mine and the Turkish speleothem So1 of Sofular cave (Figure 1, Table 2). The published chronologies of La Mine and So1 speleothems were obtained through linear interpolation between the 13 and 59 ^{230}Th dates for La Mine and So1, with 2σ uncertainties ranging between 0.17 % - 3.03 % and 0.26% - 7.53%, of ages, respectively (Genty et al., 2003, 2006; Fleitmann et al., 2009; Göktürk et al., 2011). The speleothem of La Mine grew continuously between 5.5 and 23.0 ka, and the So1 speleothem of Sofular grew nearly continuously over the last 21.2 ka (Genty et al., 2003, 2006; Fleitmann et al., 2009; Göktürk et al., 2011). Following our background parameterization, the chronologies calculated by Datice Multi-archive are then mostly constrained by the age markers with a minor influence of the prior growth rate estimations.

In figures 3 and 4, we can note that the chronologies obtained with Datice are overall in very good agreement with the published age scales of La Mine and Sofular. Compared to a simple linear regression method, which leads to constant sedimentation rates in-between markers and no uncertainty propagation (e.g. red markers on panels C of Figures 3 and 4), Datice Multi-archive produces smoother variations of the sedimentation rate with the calculation of the chronological uncertainty at all points (blue curves in figures 3 and 4). The resulting Datice Multi-archive chronology slightly differs from the published age scale of La Mine and Sofular over these intervals (panels B of Figures 3 and 4). For La Mine (Figure 3), the largest difference between the chronologies reaches about 150 years, and occurs when Datice Multi-archive does not strictly respect the absolute age of the nearby marker. The final chronology remains, however, in agreement with the absolute dates within the uncertainty range (i.e. 170 years at 12.6 ka). The difference between both chronologies is induced by the smoother evolution of age with depth with Datice Multi-archive than for the original chronology of La Mine. This difference occurs for the first marker encountered with a significantly larger uncertainty than all three previous age constraints. In such a case, Datice allows the prior estimation of the deposition rate to have more impact on the final chronology relatively to the previous, more precise, age markers. For Sofular (Figure 4), the difference between both chronologies ranges between +150 years/-300 years for Datice Multi-archive chronology. Similarly to La Mine, the largest differences between the published and the Datice Multi-archive chronologies are observed when our chronological integration tool does not strictly respect the age markers. The first large age difference of 300 years is observed at around 0.45 m from the top of the speleothem at a time when Datice Multi-archive does not respect the marker at ~6 ka, which is associated with a larger uncertainty than the surrounding ones (226 years at 1σ , against 69 years for the two closest markers). A strict fit to this age marker at ~6 ka would have induced a strong shift in the deposition

rate. Instead, Datice Multi-archive prefers to optimize and bring in agreement the chronology with the age markers presenting smaller uncertainties, preventing an abrupt change in deposition rate not primarily documented in the background estimate. Finally, the periods where the chronology uncertainties produced by Datice Multi-archive are the largest correspond to tipping periods close to a significant change in the deposition rate of calcite. In this case, Datice Multi-archive tries to reconcile the influence of two very close markers with significantly different absolute ages.

Using Datice Multi-archive to date mono-archives provides a proper assessment of the chronology uncertainty and sedimentation rate in-between the age markers. This method is more integrative than a simple linear interpolation between the age markers, **as it was implemented in the Sofular and La Mine original publications.**

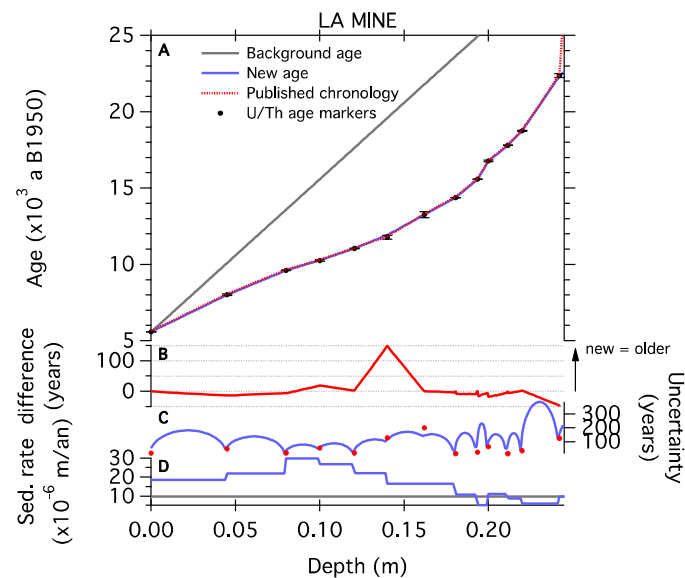


Figure 3: Comparison of chronologies for La Mine. A: depth-age relationship and age makers used to constrain the chronologies. The published chronology is in red and the new chronology obtained with Datice is in blue. B: Difference between the new chronology and the published one of Genty et al., 2006 (positive values mean that the new chronology produced by Datice is older than the published ages). C: Uncertainties of chronologies (blue for Datice, red markers for the original chronology). D: sedimentation rates. The grey curves represent the prior estimation given to Datice, the blue curves are the resulting parameters as calculated by Datice after optimization of the chronology.

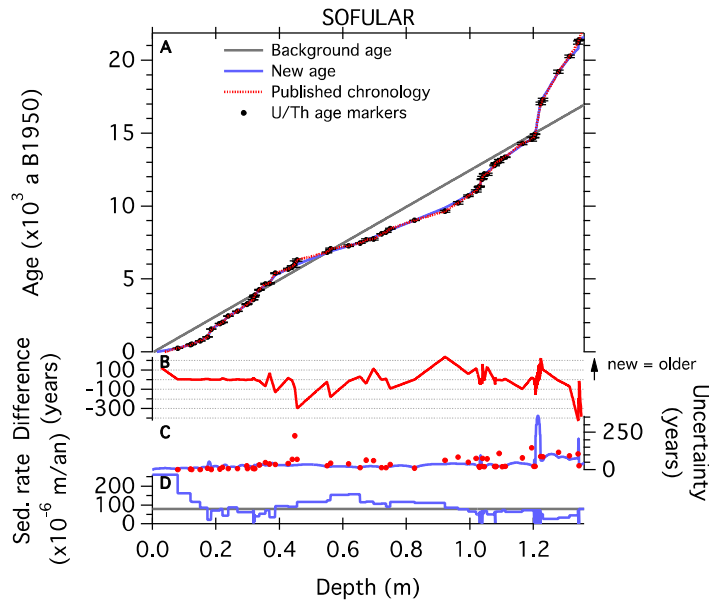


Figure 4: Same as Figure 3 for the Sofular So1 speleothem (published chronology from Fleitmann et al., 2009 and Göktürk et al., 2011).

4.2. Datice Multi-archive coherent chronology for the Mediterranean region

In this section we present the results of the Mediterranean coherent chronological framework integrating all the selected sediment/peat archives (Table 2). The chronological coherency between the different sedimentary sites is independent of any assumption of climatic alignment and only based on the identification of common and independently-dated tephra layers (Figure 2). We choose to keep the speleothem chronologies independent from the Mediterranean sediment cores in order to remain consistent and avoid unverified assumptions of climatic alignments.

The new chronology obtained with Datice for MD90-917 is in generally good agreement with the previously published chronology covering the last 24 ka (Siani et al., 2004, 2010, Figure 5). The published chronology of MD90-917 is based on 21 calibrated radiocarbon ages combined with 1 tephra layer back to 24 ka and using a simple linear regression between the markers (Siani et al., 2010, 2013). Before this period, ages were extrapolated based on the last ¹⁴C calibrated age used in this study. Compared to the published chronology, we have revised the calibration of the ¹⁴C ages into calendar ages using the IntCal13 calibration curve (Reimer et al., 2013). The largest difference between the two chronologies, up to 1115 years, is observed at the proximity of the Y3 tephra. A second significant difference occur at the proximity of the Biancavilla tephra (352 years difference at ~16.85±0.27 ka), common with Monticchio, and is induced by the combination of the tephra correlation and the revision of the ¹⁴C age marker measured just below the tephra layer. The remaining differences between the two chronologies are within the uncertainty range and can be

explained by the revision of the calibration of the ^{14}C ages and possibly the different age calculation methods (i.e. best compromise for Datice Multi-archive vs. linear interpolation for the published chronology). The close resemblance of the two chronologies confirms the reservoir ages estimates of (Siani et al., 2001) for the Adriatic Sea from the late glacial to the Holocene. The final uncertainty of MD90-917 chronology is strongly modulated by the occurrence of age markers. Indeed, the largest uncertainty values are observed at periods without age makers (e.g. ~480 years between 21-30 ka and 30-40 ka, 1σ). The new Datice Multi-archive chronology for MD90-917 is updated and more robust than the published chronology of Siani et al., 2010 over the last 24 ka, especially through providing a comprehensive estimation of the chronological uncertainty and the transfer of Monticchio's absolute constraints through the numerous stratigraphic links between the two cores.

For Monticchio, the tephra-based chronology appears a bit different from the varve-counted chronology covering the last deglaciation proposed by Allen et al. (1999), which presents an uncertainty of 5-10%. The timing of the vegetation changes corresponding roughly to the onset of the Bølling Allerød can be considered consistent within the uncertainty range of both chronologies (i.e. 15.30 ± 0.77 ka for the chronology of Allen et al., (1999) and 15.54 ± 0.14 ka for Datice Multi-archive chronology as recorded by the temperate taxa, Figure 5). However, further back in time the varve-counted chronology and the new Datice Multi-archive age scale start to significantly differ at around 18 ka (Figure 5), at the proximity of the Verdoline tephra layer and down to the bottom of the core section. Due to the correlated tephra layers, the absolute age of Monticchio is indirectly constrained by the ^{14}C calibrated ages of MD90-917 from the Tufi Biancastri ($GM1 - 14.55 \pm 0.60$ ka) back to the Pomici di base tephra (21.27 ± 0.30 ka on the new chronology), leading to older ages for this core section. The older Datice Multi-archive chronology is further confirmed and constrained by the absolutely dated Y3 tephra layer, common for all the sediment cores included here. Similarly to MD90-917, the uncertainty of the Datice Multi-archive chronology is larger when no marker constrain the chronology, e.g. up to ~500 years between 20 ka and 30 ka and up to ~680 years back to 38 ka, but remain smaller than the 5-10% estimated uncertainty of the varved chronology.

At Ohrid, the chronology of Leicher et al., (2016) was obtained after linear interpolation between the absolute ages of numerous tephra layers back to 637 ka. We used the same tephra layers to constrain our chronology over our period of interest (i.e. the Mercato, Y3 and Y5 tephras, Figure 2) with revised ages using harmonized ^{40}K decay constant and the recent ACs-2 standard for all $^{40}\text{Ar}/^{39}\text{Ar}$ dated tephra (see section 3). Both chronologies are very consistent, always in agreement within uncertainties. Moreover, similarly to the other sediment cores, the final uncertainty of the chronology tends to increase away from the age markers (Figure 5).

The original chronology of Tenaghi Philippon was obtained after the calibration of 20 ^{14}C ages from wood or peat bulk samples following the method of Weninger and Jöris (2008). The Datice Multi-archive chronology of Tenaghi Philippon is constrained with the revised ^{14}C calibrated ages proposed by Wulf et al., 2018, combined with the revised age of the Y2 tephra layer (black markers on panel D of Figure 5, Bronk Ramsey et al., 2015). The coherency of its chronology with the other Mediterranean sites is only assured at the proximity of the E1, Y3 and Y5 tephra layers (Figures 2 and 5). When comparing both chronologies, we notice two periods with major differences: ~465 years at around 16 ka and up to 1648 years between the Y3 and Y5 tephra layers. The differences for the older period most probably originate from the influence of the tephra layers and their revised absolute ages. For the younger period, it occurs between two age markers separated by ~5 ka, where the background parameter can have an influence on the final chronology. However, when considering both chronologies uncertainties, changes remain consistent.

By comparing our tephra-based coherent chronological framework with the published chronologies of each sediment site, we present the potential of Datice Multi-archive as a tool to build coherent chronologies that are common to various paleoclimate archives. The common tephra-based chronology allows us now to discuss the relative timing of changes during the last deglaciation as recorded by different proxies from multiple climate archives in the Mediterranean region.

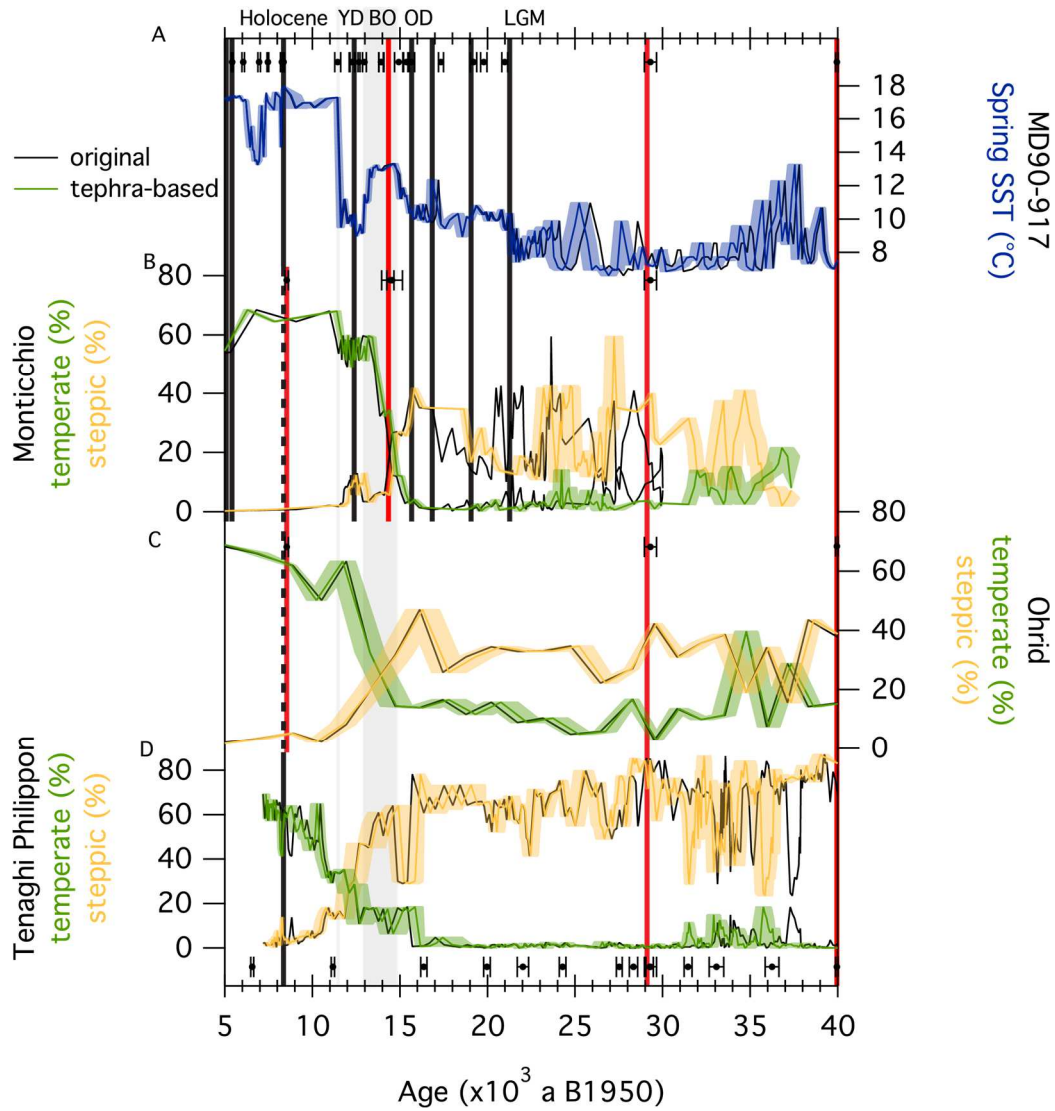


Figure 5: Comparison of chronologies between the published and the tephra-based coherent chronological framework (black lines = published, colored lines = tephra-based chronology with 1-sigma uncertainty envelopes). The positions of volcanic-based stratigraphic links are indicated by the vertical lines between the different sites. A: SST reconstruction based on planktonic foraminifera assemblages for core MD90-917 (Siani et al., 2010, 2013, this study). The top black markers indicate the position of age markers constraining its chronology. B: pollen records of Monticchio (green = temperate, orange = steppic; Allen et al., 1999). The absolute constraints for Monticchio (black markers) are present on top of the record. C: pollen records of Ohrid (green = temperate, orange = steppic; Sadori et al., 2016). Absolute constraints are represented by the black markers on top of the records. D: pollen records of Tenaghi Philippon (green = temperate, orange = steppic; Müller et al., 2011). The position of ¹⁴C calibrated age and absolutely dated markers of Tenaghi Philippon are indicated at the bottom of the records. Selected periods are indicated on top of the figure: YD for Younger Dryas (~13-11.5 ka), BO for Bølling Allerød (~15-13 ka), OD for Older Dryas (~16-15 ka) and LGM for Last Glacial Maximum.

5. Discussion: The last deglaciation in the Mediterranean region

Thanks to the different chronological constraints integrated for our different archives, we now have a coherent chronology for the sediment cores of MD90-917, Monticchio, Tenaghi Philippon and Ohrid, independent from any climatic alignment assumption. The climatic representation in the Mediterranean region is complemented here with the speleothem records of La Mine and Sofular, used to validate the development of Datice Multi-archive. It is now interesting to look at how our new coherent and improved Mediterranean chronology for the last deglaciation fits within the more global context of this transition.

The $\delta^{18}\text{O}_{\text{ice}}$ of NGRIP in Greenland records regional air temperature variability over the last glacial-interglacial cycle with an annual/seasonal resolution (NGRIP community Members, 2004). This record is dated back to 60 ka using annual layer counting (Andersen et al., 2006; Rasmussen et al., 2006; Vinther et al., 2006; Svensson et al., 2008) and is often used as a reference for comparison with new data. Compared to previous studies, we can now compare the absolute timing of changes recorded in Greenland and within the Mediterranean region independently of any alignment assumptions, thanks to our precise and coherent volcanic-based chronological framework. In figure 6, we compare the absolute timing of changes as recorded by Greenland $\delta^{18}\text{O}_{\text{ice}}$, to the Mediterranean SST reconstruction of core MD90-917 presented on the tephra-based coherent chronology, as well as La Mine and Sofular speleothems records (panels A, B, G and H of Figure 6 respectively). Consistent ages are observed for the sharp transitions recorded by the $\delta^{18}\text{O}_{\text{ice}}$ record of NGRIP and the MD90-917 SST reconstruction characterizing the Older Dryas (OD) - Bølling Allerød (BA), BA – Younger Dryas (YD) and the YD – Holocene transitions (Figure 6). The timing of changes for MD90-917 is not significantly changed when compared to its published chronology over these periods. However, the construction of the tephra-based Datice Multi-archive chronology for MD90-917 confirms the reservoir age values proposed by Siani et al., 2001 over the LGM - Holocene transition (i.e. $\sim 820 \pm 120$ years over the OD, $\sim 390 \pm 80$ years for the LGM, BA, YD and Holocene). The consistent timing of changes associated with these sharp transitions has already largely been recorded by European speleothems (Genty et al., 2006) and western Mediterranean Sea records, however relying on ^{14}C calibrations with constant reservoir ages and/or tuning to NGRIP records (Cacho et al., 2001; Martrat et al., 2004; Jiménez-Amat and Zahn, 2015). Consequently, using an independent volcanic-based age model for the Mediterranean sediment cores, we validate the general assumption of synchronous temperature changes associated with the last deglaciation over Greenland and within the Mediterranean region, independently of any climatic alignment.

Thanks to our volcanic-based coherent chronological framework, we can discuss the relative changes of vegetation between the marine core MD90-917 (Combourieu-Nebout et al., 1998, 2013),

451 Monticchio (Allen et al., 1999), Ohrid (Sadori et al., 2016) and Tenaghi Philippon (Müller et al., 2011)
 452 (panels C, D, E and F of Figure 6 respectively). With our new coherent chronological framework, we
 453 now have a proper assessment of the chronological uncertainties for each site, rendering possible
 454 the inter-comparison of relative vegetation changes between Monticchio, MD90-917, Tenaghi
 455 Philippon and Ohrid. First, all records agree in indicating a predominance of temperate taxa during
 456 the Holocene, and more steppic taxa during the last glacial period. However, the timing of changes
 457 in the predominance of temperate versus steppic pollen taxa at the different sites differs
 458 significantly and is now precisely established thanks to our multi-archive coherent chronology. At
 459 Monticchio, temperate tree taxa start to increase simultaneously with the SST increase recorded in
 460 the Adriatic Sea by the MD90-917 core, and become predominant at the onset of the Bølling-Allerød
 461 period (i.e. at 14.63 ± 0.14 ka on our coherent chronological framework). Ohrid records indicate a
 462 similar behaviour slightly later (i.e. 14.04 ± 0.87 ka), that can be considered synchronous with
 463 Monticchio within uncertainties. On the other hand, records from MD90-917 and Tenaghi Philippon
 464 show a shift in the predominance of temperate vs. steppic taxa at ~ 12 ka (i.e. at 11.98 ± 0.16 ka for
 465 MD90-917 and 12.10 ± 0.64 ka for Tenaghi Philippon). In MD90-917 records, the BA period is
 466 characterized by a dominance of steppic taxa and also higher, but still low, amounts of temperate
 467 taxa. In contrast, Monticchio and Ohrid pollen records indicate a continuous increase in temperate
 468 pollens from the initial gradual warming recorded in the Adriatic Sea until the BA-YD sharp
 469 transition. Such regional differences could originate from the difference in altitude between the
 470 sites. While MD90-917 and Tenaghi Philippon are low-altitude sites, where pollen are mostly
 471 transported by wind and basin-wide hydrological transport, Monticchio and Ohrid sites are higher in
 472 altitudes (i.e. 656 m a.s.l. for Monticchio and 693 m a.s.l. for Ohrid). They may be potentially biased
 473 by high-altitude vegetation changes and less recording vegetation changes from lower altitudes. One
 474 should note that while the temperate and steppic taxa curves present different timing of relative
 475 predominance between the four sites, the records of individual pollen species of MD90-917 (e.g.
 476 *Quercus*, *Alnus*, *Betula*) indicate an increase of trees in altitude on the mountainous slopes around
 477 the Adriatic Sea, while herb species remain dominant (e.g. *Artemisia* and *Ephedra*, Combourieu-
 478 Nebout et al., 1998). Such individual pollen behaviour is consistent with the progressive extension of
 479 forests under wetter and possibly warmer conditions during the BA than the OD, and the continuous
 480 persistence of herbs at low altitudes. Finally, the YD – Holocene transition also indicate local
 481 differences between the pollen records (Figure 6). At Monticchio, the YD-Holocene transition
 482 corresponds to a final sharp increase in the temperate pollen record, which is now concomitant with
 483 the SST and Greenland $\delta^{18}\text{O}_{\text{ice}}$ sharp changes in our tephra-based chronology. For MD90-917 and
 484 Tenaghi Philippon, the timing of this transition remains unchanged compared to the published

chronologies. Nonetheless, their pollen records present significantly different shapes in the temperate taxa records compared to Monticchio. Indeed, the YD-Holocene transition seems to be characterized by a primary increase, up to Holocene percentages in MD90-917 and halfway to Holocene amounts at Tenaghi Philippon, preceding the final shift that is synchronous with the other sites' temperature changes (Figure 6). The pollen records of Ohrid are too poorly resolved to differentiate in details the different periods characterizing the last glacial to Holocene transition. We moreover refrain from more discussion about the absolute timing of changes recorded by Tenaghi Philippon records because of the lack of stratigraphic links with the other sedimentary cores over the transition.

Depending of the local major influencing factors controlling the isotopic composition of calcite of speleothems, we can further discuss the relative changes of vegetation types based on the $\delta^{13}\text{C}_{\text{calc.}}$. Due to the geological setting of La Mine speleothem, its $\delta^{13}\text{C}_{\text{calc.}}$ record is not significantly affected by vegetation changes over the cave because today's conditions consists in a thin soil with sparse trees and bushes (Genty et al., 2006). Instead, the $\delta^{13}\text{C}_{\text{calc.}}$ at this site is more affected by changes in the soil CO_2 , which mostly results from the soil biogenic production, then indirectly from temperature and humidity conditions, and is controlled by the atmospheric CO_2 . However, it is not possible to differentiate the $\delta^{13}\text{C}_{\text{calc.}}$ of La Mine in terms of quantified changes in temperature, precipitation or CO_2 . The $\delta^{13}\text{C}_{\text{calc.}}$ of Sofular, on the other hand, is mostly influenced by the type and density of vegetation as well as the soil microbial activity over the cave (Fleitmann et al., 2009). The low values of $\delta^{13}\text{C}_{\text{calc.}}$ ($\sim -12\text{‰}$) recorded at Sofular are interpreted as a predominance of C3 plants (\sim trees) over the cave, while values around $\sim -6\text{‰}$ are associated with a predominance of C4 plants (\sim grasses).

In order to have a broader idea of vegetation changes in the Mediterranean region during the last deglaciation, we now further compare the pollen records of the integrated sediment cores against the $\delta^{13}\text{C}_{\text{calc.}}$ of Sofular, which is interpreted in terms of relative dominance of C3/trees and C4/grasses plants over the cave (located at 440 m a.s.l.). The Northwestern Turkey record of Sofular exhibits a predominance of trees during the Bølling Allerød, in agreement with the general trends of warmer and more humid conditions associated with this period. The $\delta^{13}\text{C}_{\text{calc.}}$ changes are moreover simultaneous with the sharp SST transitions recorded in the Adriatic Sea. Such a behaviour remains consistent with the interpretation of the differences between the other Mediterranean pollen records in terms of altitude sensitivity. Moreover, similarly to MD90-917 and Tenaghi Philippon, the YD – Holocene transition is associated with a two-step increase in $\delta^{13}\text{C}_{\text{calc.}}$, and the second part of the transition is synchronous with Greenland and Mediterranean SST changes. This preceding event has

517 already been recorded by other pollen and SST records within the western Mediterranean region
518 (Combourieu Nebout et al., 2009; Jiménez-Amat and Zahn, 2015).

519 While the principal transitions characterizing the last deglaciation in the Mediterranean region seem
520 to be well recorded and synchronous with Greenland changes, some differences appear in terms of
521 integrated vegetation changes between the different sites. Even if changes recorded by individual
522 vegetation species may be synchronous with temperature changes, the predominance of taxa curves
523 from one site to another may differ. These differences most probably correspond to altitudinal
524 sensitivities of vegetation species and potentially different pollen transport modes. This is especially
525 the case for sites located at high altitudes, that can remain close to shelter areas for specific species
526 over certain periods (Fleitmann et al., 2009). Inversely, pollen records from low altitude sites are
527 potentially more basin-wide integrated, and may be over-imprinted, compared to the higher-altitude
528 sites, by low-altitude pollen species. Moreover, as our tephra-based coherent chronological
529 framework evidences asynchronous changes between temperature and vegetation changes, in
530 terms of taxa dominance, within the Mediterranean region, we recommend caution when using
531 synthetic pollen records for climatic alignments with reference curves, such as SST or Greenland
532 records, to derive age models for sediment cores.

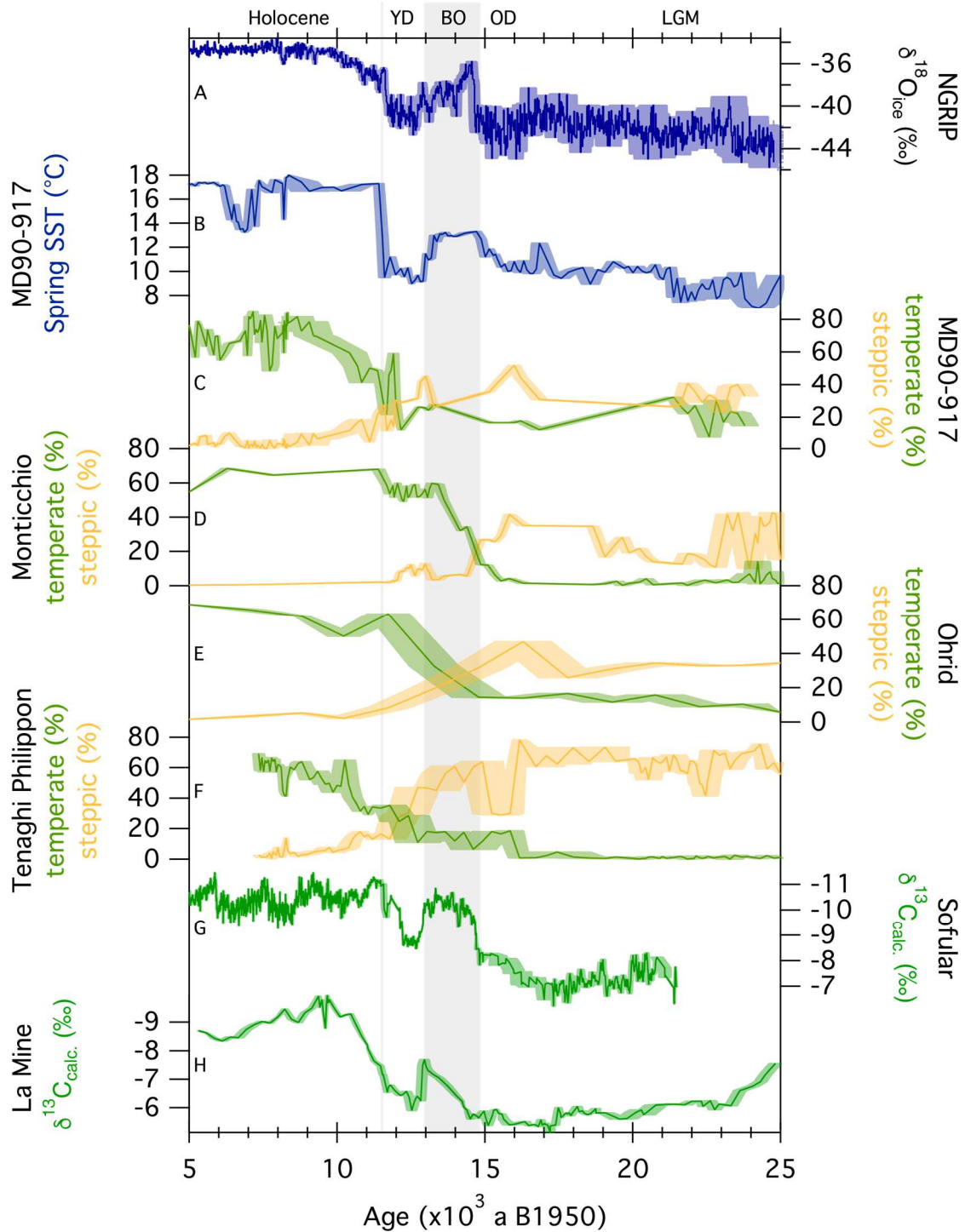


Figure 6: Comparison of the last deglaciation records, presented on the Mediterranean coherent chronology between 5 ka and 25 ka B1950, with NGRIP reference record $\delta^{18}\text{O}_{\text{ice}}$ (GICC05 chronology; NGRIP community Members, 2004). All records are presented with their respective 1σ chronological uncertainty envelope. Shaded areas highlight the position of prominent events as recorded by the SST of MD90-917 (same as in Figure 5). Selected periods are indicated on top of the figure (same as Figure 5).

Conclusion

In this paper we have presented the development and validation of Datice Multi-archive in order to build common chronologies for deposition-like archives such as speleothems or sediment records. The advantages of using Datice Multi-archive for paleoclimate studies are threefold: 1- it can simultaneously build chronologies for several sites, regardless of the type of archive (ice cores, speleothems, sediment cores), 2- it can build one single coherent and precise chronology common to all sites, and 3- it gives a proper estimation and propagation of all the chronological uncertainties. For the first time, we have validated the use of Datice Multi-archive by focusing on the last deglaciation. We combined together records from one marine core, three lake sediment cores and two independently-dated speleothems from the Mediterranean region. We have built a coherent and precise chronology based on the identification of common tephra layers between the sediment cores. Using this chronology, independent from climatic alignment assumptions, we showed that the major climatic transitions characterizing the last deglaciation were synchronous, within uncertainties, in Greenland and within the Mediterranean region. The combination of records from sediment cores and speleothems highlights local differences in terms of the timing of predominance of vegetation taxa during the last deglaciation within the Mediterranean region. However, we point to caution when combining together records from different archives and recommend a proper assessment of the parameters affecting these records prior to multi-archive data compilation and alignment of records.

Through this first multi-archive coherent chronological context, we evidence the usefulness of Datice Multi-archive for assessing the relative timing of changes between records from different climatic archives. Datice Multi-archive can be used to build coherent chronologies from regional to global scales while focusing on specific periods for different paleoclimatic applications.

Acknowledgments

We thank the two anonymous reviewers and Anders Svensson for their comments and suggestions that have helped us to improve the manuscript during the review process. This work was supported by Labex L-IPSL, which is funded by the ANR (grant no. ANR-10-LABX-0018). This work was supported by the French national program LEFE-IMAGO/INSU. This is LSCE publication number X.

Availability:

The Datice Multi-archive software is available under a CeCILL license and can be downloaded from the INRIA Forge after registration (see <https://gforge.inria.fr/account/register.php>). Documentation and support for the install of Datice Multi-archive can be found on the INRIA Forge, or upon request to lucie.bazin@lsce.ipsl.fr or lemieux.benedicte@gmail.com. The git version control tool is necessary

to clone the INRIA Forge repository. Compiling the executable requires a Fortran compiler with libraries BLAS-Lapack and netcdf (incidentally Openmp library is necessary to test the multi-threaded and shared memory beta version). Datice Multi-archive sources include the INRIA modulopt optimization solvers library (Gilbert and Jonsson, 2009). Information on how to run Datice Multi-Archive, the different input, param and output files can be found at <https://datice-multi-archives.ipsl.fr/>. A visualization tool is also available when installing Datice, requiring Python (version 2.7) with modules numpy, scipy, matplotlib, wxPython and netcdf4.

Supplementary Material:

- 1 file with all background parameters and age markers used to constrain the chronologies for all sites
- 1 file with the new Datice chronologies (depth, age, uncertainty) and data for all sites

Bibliography

- Albert, P.G., Giaccio, B., Isaia, R., Costa, A., Niespolo, E.M., Nomade, S., Pereira, A., Renne, P.R., Hinchliffe, A., 2019. Evidence for a large-magnitude eruption from Campi Flegrei caldera (Italy) at 29 ka 47, 1–5. <https://doi.org/10.1130/G45805.1/4684381/g45805.pdf>
- Albert, P.G., Hardiman, M., Keller, J., Smith, V.C., Bourne, A.J., Wulf, S., Zanchetta, G., Sulpizio, R., Müller, U.C., Pross, J., Ottolini, L., Matthews, I.P., Blockley, S.P.E., Menzies, M.A., 2015. Revisiting the Y-3 tephrostratigraphic marker: a new diagnostic glass geochemistry, age estimate, and details on its climatostratigraphical context. *Quat. Sci. Rev.* 118, 105–121. <https://doi.org/10.1016/J.QUASCIREV.2014.04.002>
- Albert, P.G., Tomlinson, E.L., Smith, V.C., Di Traglia, F., Pistolesi, M., Morris, A., Donato, P., De Rosa, R., Sulpizio, R., Keller, J., Rosi, M., Menzies, M., 2017. Glass geochemistry of pyroclastic deposits from the Aeolian Islands in the last 50 ka: A proximal database for tephrochronology. *J. Volcanol. Geotherm. Res.* 336, 81–107. <https://doi.org/10.1016/j.jvolgeores.2017.02.008>
- Allen, J.R.M., Brandt, U., Brauer, A., Hubberten, H.-W., Huntley, B., Keller, J., Kraml, M., Mackensen, A., Mingram, J., Negendank, J.F.W., Nowaczyk, N.R., Oberhänsli, H., Watts, W.A., Wulf, S., Zolitschka, B., 1999. Rapid environmental changes in southern Europe during the last glacial period. *Nature* 400, 740–743. <https://doi.org/10.1038/23432>
- Andersen, K., Svensson, A., Johnsen, S. ~J., Rasmussen, S. ~O., Bigler, M., Röthlisberger, R., Ruth, U., Siggaard-Andersen, M.-L., Peder Steffensen, J., Dahl-Jensen, D., Vinther, B. ~M., Clausen, H. ~B., 2006. The Greenland Ice Core Chronology 2005, 15 42 ka. Part 1: constructing the time scale. *Quat. Sci. Rev.* 25, 3246–3257. <https://doi.org/10.1016/j.quascirev.2006.08.002>
- Austin, W.E.N., Hibbert, F.D., 2012. Tracing time in the ocean: A brief review of chronological constraints (60-8 kyr) on North Atlantic marine event-based stratigraphies. *Quat. Sci. Rev.* 36, 28–37. <https://doi.org/10.1016/j.quascirev.2012.01.015>
- Bard, E., Arnold, M., Duprat, J., Moyes, J., Duplessy, J.-C., 1987. Reconstruction of the last

611 deglaciation: deconvolved records of $\delta^{18}\text{O}$ profiles, micropaleontological variations and
612 accelerator mass spectrometric ^{14}C dating. *Clim. Dyn.* 1, 101–112.
613 <https://doi.org/10.1007/BF01054479>

614 Barsanti, M., Delbono, I., Schirone, A., Langone, L., Miserocchi, S., Salvi, S., Delfanti, R., 2011.
615 Sediment reworking rates in deep sediments of the Mediterranean Sea. *Sci. Total Environ.* 409,
616 2959–2970. <https://doi.org/10.1016/j.scitotenv.2011.04.025>

617 Bazin, L., Landais, A., Lemieux-Dudon, B., Toyé Mahamadou Kele, H., Veres, D., Parrenin, F.,
618 Martinerie, P., Ritz, C., Capron, E., Lipenkov, V., Loutre, M.-F., Raynaud, D., Vinther, B.,
619 Svensson, A., Rasmussen, S., Severi, M., Blunier, T., Leuenberger, M., Fischer, H., Masson-
620 Delmotte, V., Chappellaz, J., Wolff, E., 2013. An optimized multi-proxies, multi-site Antarctic ice
621 and gas orbital chronology (AICC2012): 120–800 ka. *Clim. Past* 9, 1715–1731.
622 <https://doi.org/10.5194/cp-9-1715-2013>

623 Blaauw, M., Christeny, J.A., 2011. Flexible paleoclimate age-depth models using an autoregressive
624 gamma process. *Bayesian Anal.* 6, 457–474. <https://doi.org/10.1214/11-BA618>

625 Bronk Ramsey, C., 2009. BAYESIAN ANALYSIS OF RADIOCARBON DATES. *Radiocarbon* 51, 337–360.
626 <https://doi.org/10.1017/S0033822200033865>

627 Bronk Ramsey, C., Albert, P., Blockley, S., Hardiman, M., Lane, C., Macleod, A., Matthews, I.P.,
628 Muscheler, R., Palmer, A., Staff, R.A., 2014. Integrating timescales with time-transfer functions :
629 a practical approach for an INTIMATE database. *Quat. Sci. Rev.* 106, 67–80.
630 <https://doi.org/10.1016/j.quascirev.2014.05.028>

631 Bronk Ramsey, C., Albert, P.G., Blockley, S.P.E., Hardiman, M., Housley, R.A., Lane, C.S., Lee, S.,
632 Matthews, I.P., Smith, V.C., Lowe, J.J., 2015. Improved age estimates for key Late Quaternary
633 European tephra horizons in the RESET lattice. *Quat. Sci. Rev.* 118, 18–32.
634 <https://doi.org/10.1016/j.quascirev.2014.11.007>

635 Buiron, D., Chappellaz, J., Stenni, B., Frezzotti, M., Baumgartner, M., Capron, E., Landais, A., Lemieux-
636 Dudon, B., Masson-Delmotte, V., Montagnat, M., Parrenin, F., Schilt, A., 2011. TALDICE-1 age
637 scale of the Talos Dome deep ice core, East Antarctica. *Clim. Past* 7, 1–16.
638 <https://doi.org/10.5194/cp-7-1-2011>

639 Cacho, I., Grimalt, J.O., Canals, M., Sbaifi, L., Shackleton, N.J., Schönfeld, J., Zahn, R., 2001. Variability
640 of the western Mediterranean Sea surface temperature during the last 25,000 years and its
641 connection with the Northern Hemisphere climatic changes. *Paleoceanography* 16, 40–52.
642 <https://doi.org/10.1029/2000PA000502>

643 Carey, S., 1997. Influence of convective sedimentation on the formation of widespread tephra fall
644 layers in the deep sea. *Geology* 25, 839–842. [https://doi.org/10.1130/0091-7613\(1997\)025<0839:IOCSOT>2.3.CO;2](https://doi.org/10.1130/0091-7613(1997)025<0839:IOCSOT>2.3.CO;2)

646 Charbit, S., 2002. Effects of benthic transport processes on abrupt climatic changes recorded in
647 deep-sea sediments: A time-dependent modeling approach. *J. Geophys. Res.* 107, 1–19.
648 <https://doi.org/10.1029/2000jc000575>

649 Cheng, H., Edwards, R.L., Broecker, W.S., Denton, G.H., Kong, X., Wang, Y., Zhang, R., Wang, X., 2009.
650 Ice Age Terminations. *Science* (80-.). 326, 248–252. <https://doi.org/10.1126/science.1177840>

651 Clark, P.U., Shakun, J.D., Baker, P.A., Bartlein, P.J., Brewer, S., Brook, E.J., Carlson, A.E., Cheng, H.,
652 Kaufman, D.S., Lui, Z., Marchitto, T.M., Mix, A.C., Morrill, C., Otto-Bliesner, B.L., Pahnke, K.,
653 Russell, J.M., Whitlock, C., Adkins, J.F., Blois, J.L., Clark, J., Colman, S.M., Curry, W.B., Flower,

654 B.P., He, F., Johnson, T.C., Lynch-Stieglitz, J., Markgraf, V., McManus, J.F., Mitrovica, J.X.,
655 Moreno, P.I., Williams, J.W., 2012. Global climate evolution during the last deglaciation. *Proc.*
656 *Natl. Acad. Sci. U. S. A.* 109, 1134–1142. [https://doi.org/10.1073/pnas.1116619109/-](https://doi.org/10.1073/pnas.1116619109/-/DCSupplemental.www.pnas.org/cgi/doi/10.1073/pnas.1116619109)
657 [/DCSupplemental.www.pnas.org/cgi/doi/10.1073/pnas.1116619109](https://doi.org/10.1073/pnas.1116619109)

658 Combourieu-Nebout, N., Paterne, M., Turon, J.L., Siani, G., 1998. A high-resolution record of the last
659 deglaciation in the Central Mediterranean sea: Palaeovegetation and palaeohydrological
660 evolution. *Quat. Sci. Rev.* 17, 303–317. [https://doi.org/10.1016/S0277-3791\(97\)00039-5](https://doi.org/10.1016/S0277-3791(97)00039-5)

661 Combourieu-Nebout, N., Peyron, O., Bout-Roumazeilles, V., Goring, S., Dormoy, I., Joannin, S.,
662 Sadori, L., Siani, G., Magny, M., 2013. Holocene vegetation and climate changes in the central
663 Mediterranean inferred from a high-resolution marine pollen record (Adriatic Sea). *Clim. Past* 9,
664 2023–2042. <https://doi.org/10.5194/cp-9-2023-2013>

665 Combourieu Nebout, N., Peyron, O., Dormoy, I., Desprat, S., Beaudouin, C., Kotthoff, U., Marret, F.,
666 2009. Rapid climatic variability in the west Mediterranean during the last 25 000 years from
667 high resolution pollen data. *Clim. Past* 5, 503–521. <https://doi.org/10.5194/cp-5-503-2009>

668 Dansgaard, W., Johnsen, S.J., Clausen, H.B., Dahl-Jensen, D., Gundestrup, N.S., Hammer, C.U.,
669 Hvidberg, C.S., Steffensen, J.P., Sveinbjornsdottir, A.E., Jouzel, J., Bond, G., 1993. Evidence for
670 general instability of past climate from a 250-kyr ice-core record. *Nature* 364, 218–220.

671 Davies, S.M., Wastegård, S., Abbott, P.M., Barber, D.C., Bigler, M., Johnsen, S.J., Rasmussen, T.L.,
672 Steffensen, J.P., Svensson, A., 2010. Tracing volcanic events in the NGRIP ice-core and
673 synchronising North Atlantic marine records during the last glacial period. *Earth Planet. Sci.*
674 *Lett.* 294, 69–79. <https://doi.org/10.1016/j.epsl.2010.03.004>

675 Eyring, V., Bony, S., Meehl, G.A., Senior, C.A., Stevens, B., Stouffer, R.J., Taylor, K.E., 2016. Overview
676 of the Coupled Model Intercomparison Project Phase 6 (CMIP6) experimental design and
677 organization. *Geosci. Model Dev.* 9, 1937–1958. <https://doi.org/10.5194/gmd-9-1937-2016>

678 Fleitmann, D., Cheng, H., Badertscher, S., Edwards, R. ~L., Mudelsee, M., Göktürk, O. ~M.,
679 Fankhauser, A., Pickering, R., Raible, C. ~C., Matter, A., Kramers, J., Tüysüz, O., 2009. Timing and
680 climatic impact of Greenland interstadials recorded in stalagmites from northern Turkey.
681 *Geophys. Res. Lett.* 36, 19707. <https://doi.org/10.1029/2009GL040050>

682 Francke, A., Wagner, B., Just, J., Leicher, N., Gromig, R., Baumgarten, H., Vogel, H., Lacey, J.H., Sadori,
683 L., Wonik, T., Leng, M.J., Zanchetta, G., Sulpizio, R., Giaccio, B., 2016. Sedimentological
684 processes and environmental variability at Lake Ohrid (Macedonia, Albania) between 637 ka
685 and the present. *Biogeosciences* 13, 1179–1196. <https://doi.org/10.5194/bg-13-1179-2016>

686 Galli, P., Giaccio, B., Messina, P., Peronace, E., Amato, V., Naso, G., Nomade, S., Pereira, A., Piscitelli,
687 S., Bellanova, J., Billi, A., Blamart, D., Galderisi, A., Giocoli, A., Stabile, T., Thil, F., 2017. Middle
688 to Late Pleistocene activity of the northern Matese fault system (southern Apennines, Italy).
689 *Tectonophysics* 699, 61–81. <https://doi.org/10.1016/j.tecto.2017.01.007>

690 Genty, D., Blamart, D., Ghaleb, B., Plagnes, V., Causse, C., Bakalowicz, M., Zouari, K., Chkir, N.,
691 Hellstrom, J., Wainer, K., Bourges, F., 2006. Timing and dynamics of the last deglaciation from
692 European and North African $\delta^{13}\text{C}$ stalagmite profiles—comparison with Chinese and South
693 Hemisphere stalagmites. *Quat. Sci. Rev.* 25, 2118–2142.
694 <https://doi.org/10.1016/J.QUASCIREV.2006.01.030>

695 Genty, D., Blamart, D., Ouahdi, R., Gilmour, M., Baker, A., Jouzel, J., Van-Exter, S., 2003. Precise
696 dating of Dansgaard-Oeschger climate oscillations in western Europe from stalagmite data.

697 Nature 421, 833–837.

698 Giaccio, B., Niespolo, E.M., Pereira, A., Nomade, S., Renne, P.R., Albert, P.G., Arienzo, I., Regattieri,
699 E., Wagner, B., Zanchetta, G., Gaeta, M., Galli, P., Mannella, G., Peronace, E., Sottili, G.,
700 Florindo, F., Leicher, N., Marra, F., Tomlinson, E.L., 2017. First integrated tephrochronological
701 record for the last ~190 kyr from the Fucino Quaternary lacustrine succession, central Italy.
702 Quat. Sci. Rev. 158, 211–234. <https://doi.org/10.1016/j.quascirev.2017.01.004>

703 Gilbert, J.-C., Jonsson, X., 2009. An environment for testing solvers on heterogeneous collections of
704 problems. Submitt. to ACM Trans. Math. Softw.

705 Göktürk, O.M., Fleitmann, D., Badertscher, S., Cheng, H., Edwards, R.L., Leuenberger, M.,
706 Fankhauser, A., Tüysüz, O., Kramers, J., 2011. Climate on the southern Black Sea coast during
707 the Holocene: Implications from the Sofular Cave record. Quat. Sci. Rev. 30, 2433–2445.
708 <https://doi.org/10.1016/j.quascirev.2011.05.007>

709 Haslett, J., Parnell, A., 2008. A simple monotone process with application to radiocarbon-dated
710 depth chronologies. J. R. Stat. Soc. Ser. C (Applied Stat. 57, 399–418.
711 <https://doi.org/10.1111/j.1467-9876.2008.00623.x>

712 Heinrich, H., 1988. Origin and consequences of cyclic ice rafting in the Northeast Atlantic Ocean
713 during the past 130,000 years. Quat. Res. 29, 142–152. [https://doi.org/10.1016/0033-](https://doi.org/10.1016/0033-5894(88)90057-9)
714 [5894\(88\)90057-9](https://doi.org/10.1016/0033-5894(88)90057-9)

715 Imbrie, J., Imbrie, J.Z., 1980. Modeling the climatic response to orbital variations. Science 207, 943–
716 53. <https://doi.org/10.1126/science.207.4434.943>

717 Jiménez-Amat, P., Zahn, R., 2015. Offset timing of climate oscillations during the last two glacial-
718 interglacial transitions connected with large-scale freshwater perturbation. Paleoceanography
719 30, 768–788. <https://doi.org/10.1002/2014PA002710>

720 Jouzel, J., Masson-Delmotte, V., Cattani, O., Dreyfus, G., Falourd, S., Hoffmann, G., Minster, B.,
721 Nouet, J., Barnola, J.M., Chappellaz, J., Fischer, H., Gallet, J.C., Johnsen, S., Leuenberger, M.,
722 Loulergue, L., Luethi, D., Oerter, H., Parrenin, F., Raisbeck, G., Raynaud, D., Schilt, a,
723 Schwander, J., Selmo, E., Souchez, R., Spahni, R., Stauffer, B., Steffensen, J.P., Stenni, B.,
724 Stocker, T.F., Tison, J.L., Werner, M., Wolff, E.W., 2007. Orbital and millennial Antarctic climate
725 variability over the past 800,000 years. Science 317, 793–796.
726 <https://doi.org/10.1126/science.1141038>

727 Kageyama, M., Braconnot, P., Harrison, S.P., Haywood, A.M., Jungclaus, J.H., Otto-Bliesner, B.L.,
728 Peterschmitt, J.-Y., Abe-Ouchi, A., Albani, S., Bartlein, P.J., Brierley, C., Crucifix, M., Dolan, A.,
729 Fernandez-Donado, L., Fischer, H., Hopcroft, P.O., Ivanovic, R.F., Lambert, F., Lunt, D.J.,
730 Mahowald, N.M., Peltier, W.R., Phipps, S.J., Roche, D.M., Schmidt, G.A., Tarasov, L., Valdes, P.J.,
731 Zhang, Q., Zhou, T., 2018. The PMIP4 contribution to CMIP6 – Part 1: Overview and over-
732 arching analysis plan. Geosci. Model Dev. 11, 1033–1057. [https://doi.org/10.5194/gmd-11-](https://doi.org/10.5194/gmd-11-1033-2018)
733 [1033-2018](https://doi.org/10.5194/gmd-11-1033-2018)

734 Lane, C.S., Brauer, A., Blockley, S.P.E., Dulski, P., 2013. Volcanic ash reveals time-transgressive abrupt
735 climate change during the Younger Dryas. Geology 41, 1251–1254.
736 <https://doi.org/10.1130/G34867.1>

737 Lee, S., 2013. Modeling the Age of the Cape Riva (Y-2) Tephra. Radiocarbon 55, 741–747.
738 https://doi.org/10.2458/azu_js_rc.55.16214

739 Leicher, N., Zanchetta, G., Sulpizio, R., Giaccio, B., Wagner, B., Nomade, S., Francke, A., Del Carlo, P.,

2016. First tephrostratigraphic results of the DEEP site record from Lake Ohrid (Macedonia and Albania). *Biogeosciences* 13, 2151–2178. <https://doi.org/10.5194/bg-13-2151-2016>

Lemieux-Dudon, B., Bazin, L., Landais, A., Toyé Mahamadou Kele, H., Guillevic, M., Kindler, P., Parrenin, F., Martinerie, P., 2015. Implementation of counted layers for coherent ice core chronology. *Clim. Past* 11. <https://doi.org/10.5194/cp-11-959-2015>

Lemieux-Dudon, B., Blayo, E., Petit, J.R., Waelbroeck, C., Svensson, A., Ritz, C., Barnola, J.M., Narcisi, B.M., Parrenin, F., 2010. Consistent dating for Antarctic and Greenland ice cores. *Quat. Sci. Rev.* 29, 8–20. <https://doi.org/10.1016/j.quascirev.2009.11.010>

Lowe, J.J., Ramsey, C.B., Housley, R.A., Lane, C.S., Tomlinson, E.L., Stringer, C., Davies, W., Barton, N., Pollard, M., Gamble, C., Menzies, M., Rohling, E., Roberts, A., Blockley, S., Cullen, V., Grant, K., Lewis, M., MacLeod, A., White, D., Albert, P., Hardiman, M., Lee, S., Oh, A., Satow, C., Cross, J.K., Law, C.B., Todman, A., Bourne, A., Matthews, I., Müller, W., Smith, V., Wulf, S., Anghelinu, M., Antl-Weiser, W., Bar-Yosef, O., Boric, D., Boscato, P., Ronchitelli, A., Chabai, V., Veselsky, A., Uthmeier, T., Farrand, W., Gjipali, I., Ruka, R., Güleç, E., Karavanic, I., Karkanis, P., King, T., Komšo, D., Koumouzelis, M., Kyparissi, N., Lengyel, G., Mester, Z., Neruda, P., Panagopoulou, E., Shalamanov-Korobar, L., Tolevski, I., Sirakov, N., Guadelli, A., Guadelli, J.L., Ferrier, C., Skrdla, P., Slimak, L., Soler, N., Soler, J., Soressi, M., Tushabramishvili, N., Zilhão, J., Angelucci, D., Albert, P., Bramham Law, C., Cullen, V.L., Lincoln, P., Staff, R., Flower, K., Aouadi-Abdeljaouad, N., Belhouchet, L., Barker, G., Bouzouggar, A., Van Peer, P., Kindermann, K., Gerken, K., Niemann, H., Tipping, R., Saville, A., Ward, T., Clausen, I., Weber, M.J., Kaiser, K., Torksorf, J.F., Turner, F., Veil, S., Nygaard, N., Pyne-O'Donnell, S.D.F., Masojc, M., Nalepka, D., Jurochnik, A., Kabacinski, J., Antoine, P., Olive, M., Christensen, M., Bodu, P., Debout, G., Orliac, M., De Bie, M., Van Gils, M., Paulissen, E., Brou, L., Leesch, D., Hadorn, P., Thew, N., Riede, F., Heinen, M., Joris, O., Richter, J., Uthmeier, T., Knipping, M., Stika, H.P., Friedrich, M., Conard, N., Malina, M., Kind, C.J., Beutelspacher, T., Mortensen, M.F., Burdukiewicz, J.M., Szykiewicz, A., Poltowicz-Bobak, M., Bobak, D., Wisniewski, A., Przewdzicki, M., Valde-Nowak, P., Muzyczuk, A., Bramham Law, C., Cullen, V.L., Davies, L., Lincoln, P., MacLeod, A., Morgan, P., Aydar, E., çubukçu, E., Brown, R., Coltelli, M., Castro, D. Lo, Cioni, R., DeRosa, R., Donato, P., Roberto, A. Di, Gertisser, R., Giordano, G., Branney, M., Jordan, N., Keller, J., Kinvig, H., Gottsman, J., Blundy, J., Marani, M., Orsi, G., Civetta, L., Arienzo, I., Carandente, A., Rosi, M., Zanchetta, G., Seghedi, I., Szakacs, A., Sulpizio, R., Thordarson, T., Trincardi, F., Vigliotti, L., Asioli, A., Piva, A., Andric, M., Brauer, A., de Klerk, P., Filippi, M.L., Finsinger, W., Galovic, L., Jones, T., Lotter, A., Müller, U., Pross, J., Mangerud, J., Lohne, Pyne-O'Donnell, S., Markovic, S., Pini, R., Ravazzi, C., Riede, F., Theuerkauf, M., Tzedakis, C., Margari, V., Veres, D., Wastegård, S., Ortiz, J.E., Torres, T., Díaz-Bautista, A., Moreno, A., Valero-Garcés, B., Lowick, S., Ottolini, L., 2015. The RESET project: Constructing a European tephra lattice for refined synchronisation of environmental and archaeological events during the last c. 100 ka. *Quat. Sci. Rev.* 118, 1–17. <https://doi.org/10.1016/j.quascirev.2015.04.006>

Manighetti, B., McCave, I.N., Maslin, M., Shackleton, N.J., 1995. Chronology for climate change: Developing age models for the biogeochemical ocean flux study cores. *Paleoceanography* 10, 513–525. <https://doi.org/10.1029/94PA03062>

Martrat, B., Grimalt, J.O., Lopez-martinez, C., Cacho, I., Sierro, F.J., Flores, J.A., Zahn, R., Canals, M., Curtis, J.H., Hodell, D. a, 2004. Abrupt Temperature Changes in the Western Mediterranean over the Past 250,000 Years. *Science* (80-.). 306, 1762–1765. <https://doi.org/10.1126/science.1101706>

Moreno, A., Svensson, A., Brooks, S.J., Connor, S., Engels, S., Fletcher, W., Genty, D., Heiri, O., Labuhn, I., Perşoiu, A., Peyron, O., Sadori, L., Valero-Garcés, B., Wulf, S., Zanchetta, G., Allen,

787 J.R.M., Ampel, L., Blamart, D., Birks, H., Blockley, S., Borsato, A., Bos, H., Brauer, A.,
788 Combourieu-Nebout, N., de Beaulieu, J.L., Drescher-Schneider, R., Drysdale, R., Elias, S., Frisia,
789 S., Hellstrom, J.C., Ilyashuk, B., Joannin, S., Köhl, N., Larocque-Tobler, I., Lotter, A., Magny, M.,
790 Matthews, I., McDermott, F., Millet, L., Morellón, M., Neugebauer, I., Muñoz-Sobrino, C.,
791 Naughton, F., Ohlwein, C., Roucoux, K., Samartin, S., Sánchez-Goñi, M.F., Sirocko, F., van Asch,
792 N., van Geel, B., van Grafenstein, U., Vannière, B., Vegas, J., Veres, D., Walker, M., Wohlfarth,
793 B., 2014. A compilation of Western European terrestrial records 60-8kaBP: Towards an
794 understanding of latitudinal climatic gradients. *Quat. Sci. Rev.* 106, 167–185.
795 <https://doi.org/10.1016/j.quascirev.2014.06.030>

796 Müller, U.C., Pross, J., Tzedakis, P.C., Gamble, C., Kotthoff, U., Schmiedl, G., Wulf, S., Christanis, K.,
797 2011. The role of climate in the spread of modern humans into Europe. *Quat. Sci. Rev.* 30, 273–
798 279. <https://doi.org/10.1016/j.quascirev.2010.11.016>

799 NGRIP community Members, 2004. High-resolution record of Northern Hemisphere climate
800 extending into the last interglacial period. *Nature* 431, 147–151.

801 Niespolo, E.M., Rutte, D., Deino, A.L., Renne, P.R., 2017. Intercalibration and age of the Alder Creek
802 sanidine $^{40}\text{Ar}/^{39}\text{Ar}$ standard. *Quat. Geochronol.* 39, 205–213.
803 <https://doi.org/10.1016/J.QUAGEO.2016.09.004>

804 Pappalardo, L., Civetta, L., D’Antonio, M., Deino, A., Di Vito, M., Orsi, G., Carandente, A., De Vita, S.,
805 Isaia, R., Piochi, M., 1999. Chemical and Sr-isotopic evolution of the Phlegraean magmatic
806 system before the Campanian Ignimbrite and the Neapolitan Yellow Tuff eruptions. *J. Volcanol.*
807 *Geotherm. Res.* 91, 141–166. [https://doi.org/10.1016/S0377-0273\(99\)00033-5](https://doi.org/10.1016/S0377-0273(99)00033-5)

808 Parnell, A.C., Buck, C.E., Doan, T.K., 2011. A review of statistical chronology models for high-
809 resolution, proxy-based Holocene palaeoenvironmental reconstruction. *Quat. Sci. Rev.* 30,
810 2948–2960. <https://doi.org/10.1016/J.QUASCIREV.2011.07.024>

811 Parrenin, F., Bazin, L., Capron, E., Landais, A., Lemieux-Dudon, B., Masson-Delmotte, V., 2015.
812 IceChrono1: A probabilistic model to compute a common and optimal chronology for several
813 ice cores. *Geosci. Model Dev.* 8. <https://doi.org/10.5194/gmd-8-1473-2015>

814 Rasmussen, S. ~O., Andersen, K. ~K., Svensson, A. ~M., Steffensen, J. ~P., Vinther, B. ~M., Clausen, H.
815 ~B., Siggaard-Andersen, M.-L., Johnsen, S. ~J., Larsen, L. ~B., Dahl-Jensen, D., Bigler, M.,
816 Röthlisberger, R., Fischer, H., Goto-Azuma, K., Hansson, M. ~E., Ruth, U., 2006. A new
817 Greenland ice core chronology for the last glacial termination. *J. Geophys. Res.* 111, 6102.
818 <https://doi.org/10.1029/2005JD006079>

819 Reimer, P.J., Edouard Bard, B., Alex Bayliss, B., Warren Beck, B.J., Paul Blackwell, B.G., Christopher
820 Bronk Ramsey, B., 2013. Intcal13 and Marine13 Radiocarbon Age Calibration Curves 0–50,000
821 Years Cal Bp. *Radiocarbon* 55, 1869–1887.

822 Renne, P.R., Balco, G., Ludwig, K.R., Mundil, R., Min, K., 2011. Response to the comment by W.H.
823 Schwarz et al. on “Joint determination of ^{40}K decay constants and $^{40}\text{Ar}^*/^{40}\text{K}$ for the Fish
824 Canyon sanidine standard, and improved accuracy for $^{40}\text{Ar}/^{39}\text{Ar}$ geochronology” by P.R. Renne
825 et al. (2010). *Geochim. Cosmochim. Acta* 75, 5097–5100.
826 <https://doi.org/10.1016/J.GCA.2011.06.021>

827 Sadori, L., Koutsodendris, A., Panagiotopoulos, K., Masi, A., Bertini, A., Combourieu-Nebout, N.,
828 Francke, A., Kouli, K., Joannin, S., Mercuri, A.M., Peyron, O., Torri, P., Wagner, B., Zanchetta, G.,
829 Sinopoli, G., Donders, T.H., 2016. Pollen-based paleoenvironmental and paleoclimatic change
830 at Lake Ohrid (south-eastern Europe) during the past 500 ka. *Biogeosciences* 13, 1423–1437.

831 <https://doi.org/10.5194/bg-13-1423-2016>

832 Shakun, J.D., Clark, P.U., He, F., Marcott, S.A., Mix, A.C., Liu, Z., Otto-Bliesner, B., Schmittner, A.,
833 Bard, E., 2012. Global warming preceded by increasing carbon dioxide concentrations during
834 the last deglaciation. *Nature* 484, 49–54. <https://doi.org/10.1038/nature10915>

835 Siani, G., Magny, M., Paterne, M., Debret, M., Fontugne, M., 2013. Geoscientific Instrumentation
836 Methods and Data Systems Paleohydrology reconstruction and Holocene climate variability in
837 the South Adriatic Sea. *Clim. Past* 9, 499–515. <https://doi.org/10.5194/cp-9-499-2013>

838 Siani, G., Paterne, M., Colin, C., 2010. Late glacial to Holocene planktic foraminifera bioevents and
839 climatic record in the South Adriatic Sea. *J. Quat. Sci.* 25, 808–821.
840 <https://doi.org/10.1002/jqs.1360>

841 Siani, G., Paterne, M., Michel, E., Sulpizio, R., Sbrana, A., Arnold, M., Haddad, G., 2001.
842 Mediterranean Sea surface radiocarbon reservoir age changes since the last glacial maximum.
843 *Science* 294, 1917–20. <https://doi.org/10.1126/science.1063649>

844 Siani, G., Sulpizio, R., Paterne, M., Sbrana, A., 2004. Tephrostratigraphy study for the last 18,000 14C
845 years in a deep-sea sediment sequence for the South Adriatic. *Quat. Sci. Rev.* 23, 2485–2500.
846 <https://doi.org/10.1016/J.QUASCIREV.2004.06.004>

847 Svensson, A., Andersen, K.K., Bigler, M., Clausen, H.B., Dahl-Jensen, D., Davies, S.M., Johnsen, S.J.,
848 Muscheler, R., Parrenin, F., Rasmussen, S.O., Röthlisberger, R., Seierstad, I., Steffensen, J.P.,
849 Vinther, B.M., 2008. A 60 000 year Greenland stratigraphic ice core chronology. *Clim. Past* 4,
850 47–57. <https://doi.org/10.5194/cp-4-47-2008>

851 Tomlinson, E.L., Albert, P.G., Wulf, S., Brown, R.J., Smith, V.C., Keller, J., Orsi, G., Bourne, A.J.,
852 Menzies, M.A., 2014. Age and geochemistry of tephra layers from Ischia, Italy: Constraints from
853 proximal-distal correlations with Lago Grande di Monticchio. *J. Volcanol. Geotherm. Res.* 287,
854 22–39. <https://doi.org/10.1016/j.jvolgeores.2014.09.006>

855 Tomlinson, E.L., Arienzo, I., Civetta, L., Wulf, S., Smith, V.C., Hardiman, M., Lane, C.S., Carandente, A.,
856 Orsi, G., Rosi, M., Müller, W., Menzies, M.A., 2012. Geochemistry of the Phlegraean Fields
857 (Italy) proximal sources for major Mediterranean tephras: Implications for the dispersal of
858 Plinian and co-ignimbritic components of explosive eruptions. *Geochim. Cosmochim. Acta* 93,
859 102–128. <https://doi.org/10.1016/j.gca.2012.05.043>

860 Veres, D., Bazin, L., Landais, A., Tøye Mahamadou Kele, H., Lemieux-Dudon, B., Parrenin, F.,
861 Martinerie, P., Blayo, E., Blunier, T., Capron, E., Chappellaz, J., Rasmussen, S., Severi, M.,
862 Svensson, A., Vinther, B., Wolff, E., 2013. The Antarctic ice core chronology (AICC2012): an
863 optimized multi-parameter and multi-site dating approach for the last 120 thousand years.
864 *Clim. Past* 9, 1733–1748. <https://doi.org/10.5194/cp-9-1733-2013>

865 Vinther, B. ~M., Clausen, H. ~B., Johnsen, S. ~J., Rasmussen, S. ~O., Andersen, K. ~K., Buchardt, S. ~L.,
866 Dahl-Jensen, D., Seierstad, I. ~K., Siggaard-Andersen, M.-L., Steffensen, J. ~P., Svensson, A.,
867 Olsen, J., Heinemeier, J., 2006. A synchronized dating of three Greenland ice cores throughout
868 the Holocene. *J. Geophys. Res.* 111, 13102. <https://doi.org/10.1029/2005JD006921>

869 Weninger, B., Jöris, O., 2008. A 14C age calibration curve for the last 60 ka: the Greenland-Hulu U/Th
870 timescale and its impact on understanding the Middle to Upper Paleolithic transition in
871 Western Eurasia. *J. Hum. Evol.* 55, 772–781. <https://doi.org/10.1016/J.JHEVOL.2008.08.017>

872 Wulf, S., Hardiman, M.J., Staff, R.A., Koutsodendris, A., Appelt, O., Blockley, S.P.E., Lowe, J.J.,
873 Manning, C.J., Ottoloni, L., Schmitt, A.K., Smith, V.C., Tomlinson, E.L., Vakhrameeva, P.,

874 Knipping, M., Kotthoff, U., Milner, A.M., Müller, U.C., Christanis, K., Kalaitzidis, S., Tzedakis,
875 P.C., Schmiedl, G., 2018. The marine isotope stage 1 e 5 cryptotephra record of Tenaghi
876 Philippon , Greece : Towards a detailed tephrostratigraphic framework for the Eastern
877 Mediterranean region 186, 236–262. <https://doi.org/10.1016/j.quascirev.2018.03.011>

878 Wulf, S., Kraml, M., Brauer, A., Keller, J., Negendank, J.F.W., 2004. Tephrochronology of the 100ka
879 lacustrine sediment record of Lago Grande di Monticchio (southern Italy). *Quat. Int.* 122, 7–30.
880 <https://doi.org/10.1016/j.quaint.2004.01.028>

881 Wulf, S., Kraml, M., Keller, J., 2008. Towards a detailed distal tephrostratigraphy in the Central
882 Mediterranean: The last 20,000 yrs record of Lago Grande di Monticchio. *J. Volcanol.*
883 *Geotherm. Res.* 177, 118–132. <https://doi.org/10.1016/j.jvolgeores.2007.10.009>

884 Zanchetta, G., Sulpizio, R., Roberts, N., Cioni, R., Eastwood, W.J., Siani, G., Caron, B., Paterne, M.,
885 Santacroce, R., 2011. Tephrostratigraphy, chronology and climatic events of the Mediterranean
886 basin during the Holocene: An overview. *Holocene* 21, 33–52.
887 <https://doi.org/10.1177/0959683610377531>

888